Multi-Ligand-Binding Flavoprotein Dodecin as a Key Element for Reversible Surface Modification in Nano-biotechnology

Cristina Gutiérrez Sánchez,[†] Qiang Su,[†] Holger Schönherr,[‡,§] Martin Grininger,[∥] and Gilbert Nöll*[,†]

[†]Nöll Junior Research Group, Organic Chemistry, Department of Chemistry and Biology, [‡]Physical Chemistry I, Department of Chemistry and Biology, and [§]Research Center of Micro and Nanochemistry and Engineering (Cμ), University of Siegen, Adolf-Reichwein-Straße 2, 57076 Siegen, Germany and [∥]Goethe University Frankfurt, Riedberg Campus FMLS Building, Max-von-Laue Straße 15, 60438 Frankfurt am Main, Germany

ABSTRACT In this paper the multiple (re)programming of protein—DNA nanostructures comprising generation, deletion, and reprogramming on the same flavin-DNA-modified surface is introduced. This work is based on a systematic study of the binding affinity of the multi-ligand-binding flavoprotein dodecin on flavin-terminated DNA monolayers by surface plasmon resonance and quartz crystal microbalance with dissipation (QCM-D) measurements, surface plasmon fluorescence spectroscopy (SPFS), and dynamic AFM force spectroscopy. Depending on the flavin surface coverage, a single apododecin is captured by one or more surface-immobilized flavins. The corresponding complex binding and unbinding rate constants $k_{on(QCM)} = 7.7 \times 10^3\ M^{-1} \cdot s^{-1}$ and $k_{off(QCM)} = 4.5 \times 10^{-3}\ s^{-1}$ ($K_{d(QCM)} = 580$ nM) were determined by QCM and were found to be in agreement with values for k_{off} determined by SPFS and force spectroscopy. Even though a single apododecin—flavin bond is relatively weak, stable dodecin monolayers were formed on flavin-DNA-modified surfaces at high flavin surface coverage due to multivalent interactions between apododecin bearing six binding pockets and the surface-bound flavin-DNA ligands. If bi- or multivalent flavin ligands are adsorbed on dodecin monolayers, stable sandwich-type surface-DNA-flavin-apododecin-flavin ligand arrays are obtained. Nevertheless, the apododecin flavin complex is easily and quantitatively disassembled by flavin reduction. Binding and release of apododecin are reversible processes, which can be carried out alternatingly several times to release one type of ligand by an external redox trigger and subsequently replace it with a different ligand. Hence the versatile concept of reprogrammable functional biointerfaces with the multi-ligand-binding flavoprotein dodecin is demonstrated.

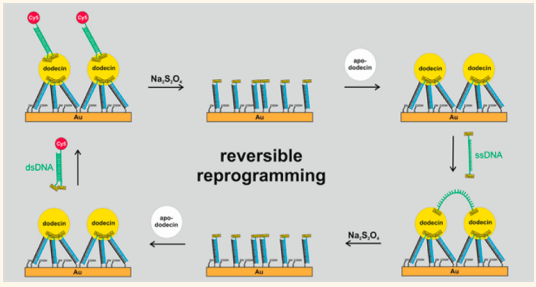

KEYWORDS: dodecin · flavins and flavoproteins · multidentate ligands · multiple or multivalent binding · QCM-D · SPR

In recent years there is growing interest in the development of smart surfaces for applications in nano-biotechnology.[1−6] The properties of these surfaces can be switched by external stimuli such as the pH, temperature, light, electrochemical potential, enzymatic reactions, or ligand binding.[1−6] For the generation of smart surfaces even switchable guest—host systems have been engineered.[7,8] In this contribution the multi-ligand-binding flavoprotein dodecin is introduced as a key element for surface modification in nano-biotechnology, which allows the multiple generation, erasure, and reprogramming of surface architectures. Dodecin from *Halobacterium salinarum* is a dodecameric hollow-spherical riboflavin-binding protein with a diameter of about 7 nm.[9−16] Dodecin comprises six binding pockets with octahedral arrangement. Each dodecin binding pocket can bind up to two flavin ligands. Hence, dodecin is able to bind up to 12 flavins in total. Dodecin binds not only native but also artificial flavins such as flavin-DNA tethers with high affinity if the flavins are oxidized, whereas flavin reduction induces the dissociation of the holoprotein in apododecin and free flavin ligands.[9,13,15] For a single dodecin—flavin bond the dissociation constant (K_d) determined by a fluorescence quenching binding assay was found to be in the nanomolar range.[9,13,15] Further studies to elucidate the

* Address correspondence to noell@chemie.uni-siegen.de.

Received for review December 8, 2014 and accepted March 4, 2015.

Published online March 04, 2015
10.1021/nn506993s

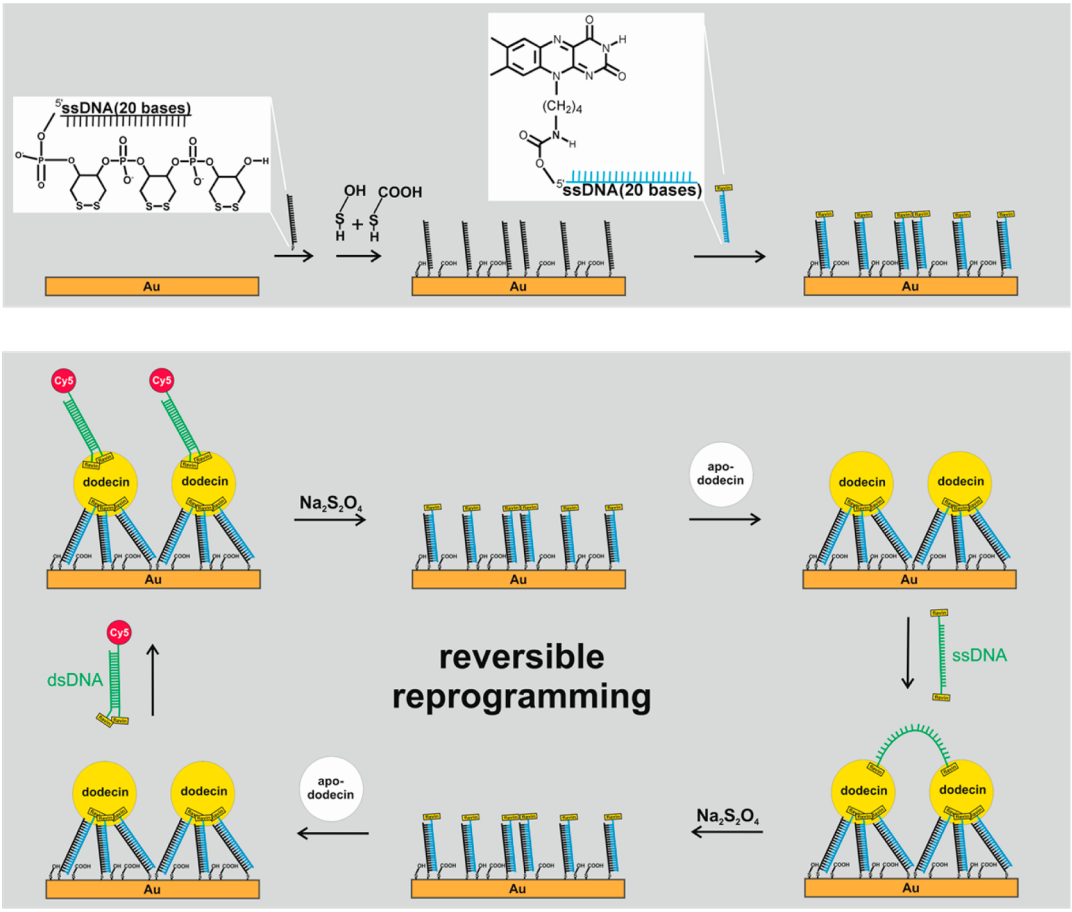

Scheme 1. (Top) Strategy for the generation of a flavin-modified dsDNA layer. (Bottom) The flavin-modified dsDNA layer is used for the binding of apododecin and bidentate flavin-DNA ligands (writing). After disassembly of the surface architecture by chemical flavin reduction (erasure) the flavin-modified dsDNA layer can be used for further writing and erasure cycles. Multiple reprogramming using different bidentate flavin-DNA ligands is possible.

binding kinetics and/or cooperative binding effects involving individual binding sites have not been carried out until now. Here we present the first detailed study of the binding affinity of the multivalent tE variant of apododecin (DtE) for flavin ligands attached to a surface by surface plasmon resonance (SPR), surface plasmon fluorescence spectroscopy (SPFS), and quartz crystal microbalance with dissipation mode (QCM-D) measurements. The flavin ligands were attached to a gold surface by thiol-anchored double-stranded DNA (dsDNA) tethers of 20 base pairs (bp).[9,15] In order to form the flavin-modified DNA layer on gold, a stepwise surface modification procedure, as depicted in Scheme 1, was carried out. In adsorption/desorption studies we monitor the time-dependent mass uptake/loss due to association/dissociation of the holoprotein complex formed between surface-tethered flavins and free DtE in buffer solution (buffer A, see Materials section in the Supporting Information).

By fitting the kinetic data to the Langmuir model the binding/unbinding rate constants (k_{on}/k_{off}) can be calculated.[17−20] Based on the results of the binding affinity studies, a strategy for the use of the DtE−flavin system as a tool for reversible surface modification in nano-biotechnology is developed as shown in Scheme 1. For this purpose we use the concept of multivalency for the generation of protein−DNA surface architectures with extended long-term stability. Bidentate flavin-DNA ligands of different structure and flexibility are compared with respect to their ability to bind to apododecin monolayers with increased affinity. Furthermore, we show that sandwich-type flavin-apododecin-flavin surface architectures can be generated and afterward disassembled by flavin reduction; multiple erasure and reprogramming of the surface architectures is possible.

RESULTS AND DISCUSSION

In order to modify the gold-coated sensor chips with flavins, single-stranded DNA equipped with three dithiane groups was adsorbed onto precleaned gold surfaces in 20 mM tris-buffer at pH 7.5 containing 1 M NaCl and 5 mM $MgCl_2$ (for detailed structures of the DNA strands see Supporting Information, Chart S1).[9,15] Three dithiane rings forming six sulfur−gold bonds were used for chemisorption on gold, since it has been shown that oligonucleotides, which have been chemisorbed by six thiol anchors, are stable against displacement even at high salt concentration, at elevated

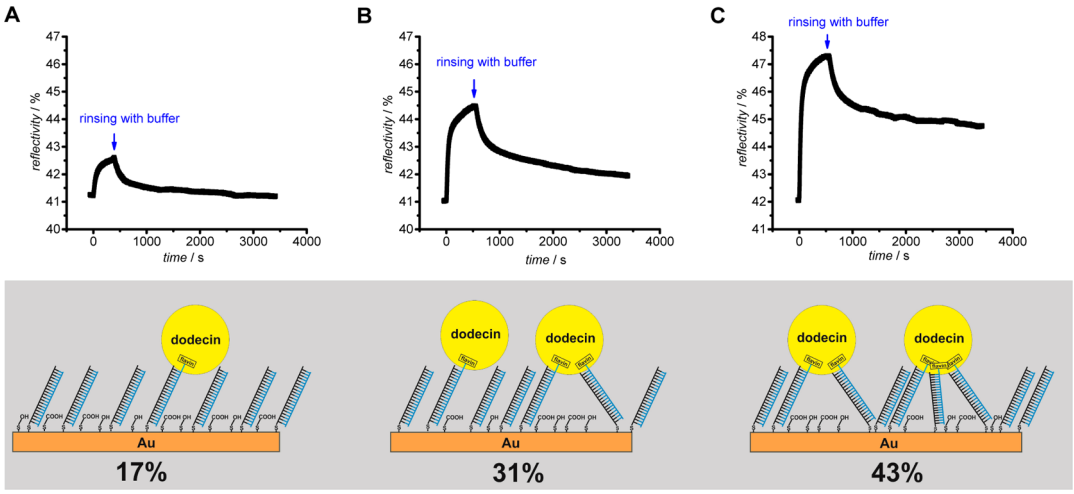

Figure 1. SPR kinetic scan curves showing the adsorption/desorption kinetics of apododecin DtE *via* single/multiple binding events with flavin ligands. The relative flavin surface coverages were 17% (A), 31% (B), and 43% (C). The cartoon below shows the increased contribution of secondary binding events along with increased flavin ligand concentration, explaining the changes in DtE binding/unbinding kinetics.

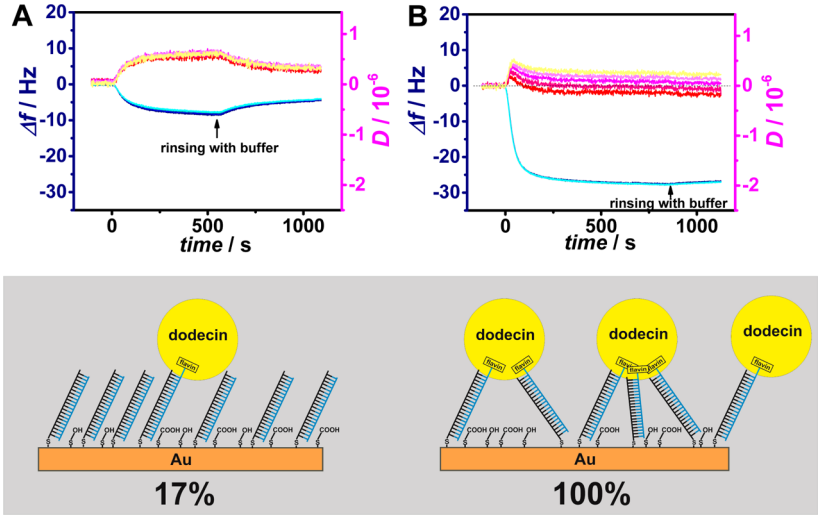

Figure 2. Frequency (blue) and dissipation (red) shifts (overtones 5−13) observed *in situ* by QCM for adsorption/desorption of apododecin DtE on surfaces modified with two different surface coverages of flavin ligands: (A) 17% and (B) 100%.

temperature, or in the presence of alkaline solution (in contrast to monofunctional thiol-terminated oligonucleotides).[21] In the next step a mixture of mercaptobutanol (MCB) and mercaptopropionic acid (MPA) in water was incubated in order to release nonspecifically adsorbed DNA and patch any unmodified areas exposing bare gold.[9,15] After rinsing with buffer, complementary flavin-modified ssDNA was added for hybridization.[9,15] This resulted in a relative flavin surface coverage of 100% with respect to the surface-tethered dsDNA. We used a mixture of MCB and MPA (1:1) as spacers between individual oligonucleotides, since these relatively short thiols do not hamper the hybridization event. In a previous study on surface-bound molecular beacons (which were chemisorbed by three dithiane groups as well) we have shown that by using these spacers stable oligonucleotide layers can be formed on gold, and several hybridization/dehybridization steps can be carried out without any decrease in efficiency.[22] In order to investigate different flavin surface coverages at the same ssDNA-modified sensor chip, dehybridization of the complementary ssDNA (drawn in blue in Figures 1 and 2) was induced by rinsing with pure water, before a mixture with different ratios between flavin-modified and flavin-free complementary ssDNA was added. Thus, the same surface architecture with constant dsDNA concentration was obtained, whereas the concentration of the flavin end groups varied. Hence three surfaces with different flavin surface coverages were prepared and subsequently investigated by SPR during the adsorption of DtE and the subsequent rinsing with pure buffer solution (desorption). The corresponding SPR kinetic scan curves (see Figure 1) revealed that an increase in the flavin ligand concentration results in larger amounts of adsorbed DtE.

Desorption of the apoprotein upon rinsing with buffer showed that the kinetics differ from monoexponential kinetics for higher contents of the flavin ligands. The latter is expected for a protein layer formed exclusively by primary or monovalent binding events (one apododecin binds one flavin ligand). Since a single DtE molecule comprising six flavin binding pockets can be bound by several linkages in parallel, we explain the observed unbinding kinetics by an increasing fraction of secondary or tertiary binding events (individual apododecin DtE molecules bind two or three flavin ligands) depending on the flavin surface coverage as shown in the scheme in Figure 1. For the sample with low surface concentration of flavin ligands (17%), the contribution from secondary binding events is low (for details see Figure S3D in the Supporting Information), whereas at higher flavin surface coverage (31% and 43%) multiple binding events become more and more frequent. In order to estimate the maximum amount of apododecin that can be bound to a flavin-terminated DNA monolayer, angular SPR scan curves were measured before and after apododecin DtE adsorption on three identically prepared SPR chips with a flavin surface coverage of 100%. From the shifts observed an average optical thickness ($n \times d$) of the apododecin monolayer of 3.9 nm was determined. Assuming a refractive index of $n = 1.50$ for apododecin, an average layer thickness of 2.6 nm can be calculated. As the diameter of apododecin DtE is about 7 nm, this value for the layer thickness implies that a partial monolayer is formed. In a control experiment DtE showed no binding affinity to a layer of pristine dsDNA (without flavin ligands). Thus, the DNA layer creates an efficient barrier to prevent nonspecific DtE adsorption.

Analogous results were obtained in QCM measurements (see Figure 2). At 100% flavin surface coverage (Figure 2B), multiple binding results in the formation of a stable monolayer of biospecifically adsorbed protein molecules, and extended rinsing has no noticeable effect on its integrity. Due to the octahedral arrangement of the six dodecin binding pockets, up to three binding pockets should be accessible for each apododecin molecule approaching the flavin-modified surface. Nevertheless, when the adsorbed proteins form a monolayer and neighboring molecules in this layer experience steric repulsion, the likelihood of secondary binding events decreases. Therefore, immediately upon rinsing, we observe a minor decrease of the adsorbed amount, which can be explained by desorption of the small fraction of protein molecules, which are presumably attached *via* single linkages. At low flavin surface coverages (17% in Figure 2A), the majority of the apododecin molecules were bound to either one or, possibly, two ligands.

According to the results of the QCM dissipation measurements, the adsorption of apododecin starts with a fast increase of the dissipation signal followed by its sudden decrease upon further adsorption for the sample with 100% flavin (Figure 2B). Such behavior is often observed for heterogeneous adsorption layers, and it was thoroughly investigated for adsorption of globular proteins.[23−27] The increase of the dissipation signal in these systems was related to the mechanical compliance of the binding tether. The soft sublayer allows rocking and sliding motions of the adsorbed particles, thus providing the major source of the bandwidth shift.[25] However, at high degrees of surface coverage, lateral motion of the adsorbed particles is being restricted, which results in a lower dissipation of the acoustic waves.[24] This model explains the presence of the transient peak in the dissipation signal observed upon adsorption of the spherical apododecin molecules on the surface with flavin-dsDNA ligands (Figure 2B). The fact that dissipation values for lower overtones decrease below the initial level (compared to the signal before the protein was adsorbed) is related to the lateral motion of the DNA double helices,[28,29] which is also being restricted upon binding with apododecin.

As previously mentioned, the geometry of apododecin, characterized by the octahedral allocation of the six binding pockets, allows the formation of up to three linkages with flavin ligands attached to the substrate surface *via* the dsDNA tethers with 20 bp. Upon binding of the multivalent apododecin with three flavin-dsDNA ligands, we obtain a relatively stiff structural unit on the surface. The overall rigidity of the surface film is indicated by the low ratio of dissipation *versus* frequency shift (*Df* ratio) and no noticeable spreading of the frequency overtones. Considerable spreading of the dissipation overtones, on the other hand, is a characteristic behavior commonly observed for heterogeneous films.[25] For samples with low concentration of flavin ligands, we observed a high ratio of dissipation *versus* frequency shift upon adsorption of apododecin (Figure 2A). In this case, the majority of the adsorbed DtE molecules are bound *via* a single flavin-DNA tether and the obtained structure is not restricted in lateral motion. Mechanical compliance of the tether with the attached protein molecule results in the formation of a viscous layer, which is also indicated by (minor) spreading of the frequency overtones (an enlarged presentation of the frequency shifts depicted in Figure 2A is shown in the Supporting Information, Figure S1).[30] Analogous to SPR the QCM-D measurements show that even at a relatively low flavin surface coverage secondary binding events have to be taken into account, while at higher flavin surface coverage the protein monolayer is highly stabilized by multiple binding.[31−35]

In order to determine the binding/unbinding rate constants (k_{on}/k_{off}) from QCM measurements, the flavin surface coverage was further reduced to minimize

the probability for multiple binding to occur. As shown in the Supporting Information (Figure S2), average values of $k_{on(QCM)} = 7.7 \times 10^3\ M^{-1} \cdot s^{-1}$ and $k_{off(QCM)} = 4.5 \times 10^{-3}\ s^{-1}$ were obtained from the kinetic QCM curves collected for a flavin surface coverage of 10%. From these values a dissociation constant of $K_{d(QCM)} = 580$ nM was calculated, which is in good agreement with a value of $K_d = 400$ nM determined by a fluorescence-quenching binding assay (in solution) for DtE with flavin (CofC4)-DNA ligands with five bases.[15] During the SPR measurements at flavin surface coverages of 15% or less, the signal-to-noise ratio did not allow for an accurate determination of the k_{on} and k_{off} values (see Supporting Information, Figure S3).

The binding and release of a monodentate fluorophore-labeled flavin-dsDNA ligand on a DtE monolayer could also be unraveled in SPFS measurements, in which a value of $k_{off(SPFS)} = 1.6 \times 10^{-3}\ s^{-1}$ was determined (see Supporting Information, Figure S4). In the Supporting Information (Figure S5) we show further that a DtE monolayer with high long-term stability can be formed by using flavin-DNA tethers with a flavin surface coverage of 100%. In addition we show by QCM measurements that, while a dodecin monolayer formed by using flavin-DNA tethers with a flavin surface coverage of 100% is stable upon extended rinsing with buffer solution for hours (see Figure S5), the apododecin–flavin complex can be disassembled quantitatively and reversibly by chemical flavin reduction (see Figure S6). The same observation has been made previously by SPR, when electron transfer through DNA monolayers was investigated.[15] A k_{off} value on the same order of magnitude as determined by QCM and SPFS, $k_{off(AFM)} = 6.8 \times 10^{-3}\ s^{-1}$, was obtained by dynamic AFM spectroscopy (see Supporting Information, Figure S8).[36−39] By comparing the values for k_{off} and K_d of DtE–flavin with those of streptavidin–biotin, which shows an extraordinarily high binding affinity and is thus often used for surface modification in nano-biotechnology in sandwich type assays,[40−45] it turns out that a single DtE–flavin bond is too weak for permanent attachment of flavin ligands to dodecin-modified surfaces. This can easily be estimated by comparing the half-lifes $\tau > 50$ h for a streptavidin–biotin ($k_{off} = 3.8 \times 10^{-6}\ s^{-1}$) (compare ref 17) and $\tau = 2$–10 min for a dodecin–flavin bond (depending on the exact value of k_{off}).

On the other hand, it should be possible to significantly increase the binding strength of flavin-modified ligands, if the concept of multivalent binding is applied, *i.e.*, if bi- or multidentate ligands are used.[31−35,46,47] In Figure 3 we compare the binding strength of a mono- and bidentate fluorophore-labeled flavin-dsDNA ligand (**Bi1**) adsorbed to a dodecin DtE monolayer upon extended rinsing with buffer solution by SPFS. For comparison also the fluorescence signal caused by a nonbinding (flavin-free) fluorophore-labeled ssDNA

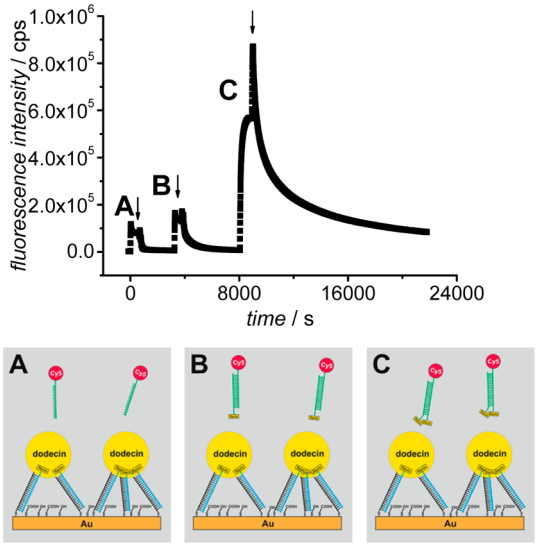

Figure 3. SPFS kinetic scan curve collected during ligand addition and subsequent rinsing with buffer (start of rinsing is indicated by arrows) for a Cy5-labeled nonbinding (flavin-free) ssDNA ligand (A), a Cy5-labeled monodentate flavin-dsDNA ligand (B), and a Cy5-labeled bidentate flavin-dsDNA ligand Bi1 (C) at a dodecin DtE monolayer (prepared with 100% flavin surface coverage). In the scan curve there is an additional signal increase (and decrease) when the peristaltic pump was switched on (and off).

ligand was measured, since there is an additional fluorescence signal by filling the flow cell with a fluorophore-containing solution. After addition of the nonbinding ligand (Figure 3A) the fluorescence signal decreases as soon as the ligand-containing solution is removed from the cell. While the vast majority of the monodentate ligand could be removed after less than 1 h of rinsing with buffer (Figure 3B), a significant amount of bidentate ligands **Bi1** remains bound to the dodecin monolayer even after rinsing for more than 3 h (Figure 3C).

The same experiment shown in Figure 3 was repeated using QCM-D. During the addition of the nonbinding ssDNA ligand no significant change in frequency could be observed. The frequency shift collected during the addition of the monodentate flavin-dsDNA ligand was small (about −1 Hz), and the initial level was reached after rinsing for about 50 min (data not shown).

The QCM-D curve measured during binding of the bidentate flavin-dsDNA ligand **Bi1** and subsequent rinsing is shown in Figure 4. Also from the QCM-D measurements it can be seen that the overall binding strength for the bidentate dsDNA ligand is significantly increased in comparison to the monodentate ligand. After rinsing for more than 1 h, about 50% of the bidentate ligand **Bi1** stayed captured at the surface. Fitting the binding and unbinding kinetics of ligand **Bi1** shown in Figure 4 revealed two kinetic regimes (for details see Supporting Information, Figure S9). Apparently some of the bidentate ligand molecules

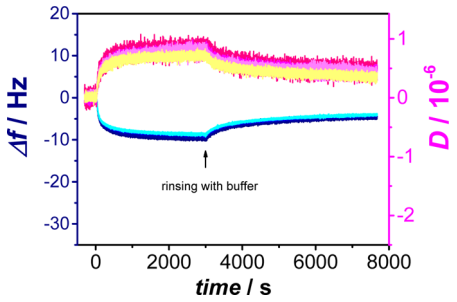

Figure 4. Frequency (blue) and dissipation (red) shifts (overtones 5−13) for adsorption/desorption of the Cy5-labeled bidentate flavin-dsDNA ligand Bi1 at a dodecin DtE monolayer (prepared with 100% flavin surface coverage).

were bound only by one of the two flavins. At this point it is worth mentioning that the previously determined binding/unbinding rate constants (k_{on}/k_{off}) for the apododecin−flavin system describe the binding of a single flavin-DNA ligand at one of the two accessible sites of one of the six dodecin binding pockets. For small flavin ligands it is expected that the second binding event may occur also with higher affinity, because the isoalloxazine moieties of both flavin ligands will then be arranged in an aromatic tetrad together with two tryptophanes being part of the apoprotein. The formation of the aromatic tetrad is expected to increase the overall stability of the complex due to electronic interaction.[9,13,15] In the case of rather bulky flavin-DNA ligands on the other hand, the binding of the second ligand in the same pocket could be hampered for steric reasons and might thus occur with lower affinity. For the bidentate dsDNA ligand **Bi1** both flavin ligands are attached to the same end of the dsDNA, and the length of the linkers used for 3′ and 5′ modification is not exactly the same. When the rather bulky bidentate dsDNA ligand **Bi1** is bound, both flavins have to be incorporated into the same dodecin binding pocket, which may result in steric constraints limiting the overall binding efficiency. Therefore, we decided to investigate another bidentate ligand, **Bi2**, consisting of ssDNA with 20 bases equipped with flavins on both ends (the 3′ and the 5′ end). Due to the high flexibility of the ssDNA, both flavins of this ligand can be bound to the same binding pocket of a single DtE molecule, to two different binding pockets of the same DtE molecule, or to two binding pockets belonging to different DtE molecules. In Figure 5 the binding/unbinding kinetics of the new bidentate flavin-ssDNA ligand **Bi2** are shown. After rinsing for almost 1 h the vast majority of the ligand molecules remain captured at the surface. Apparently the more flexible structure of ligand **Bi2** allows both flavins to approach the most convenient binding positions in combination with each other. A detailed analysis of the binding and unbinding kinetics of ligand **Bi2** is provided in the Supporting Information, Figure S10.

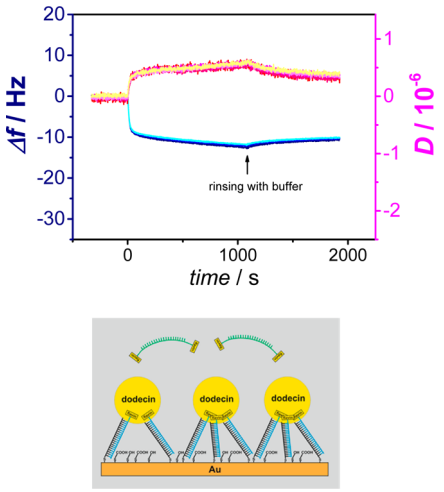

Figure 5. QCM frequency (blue) and dissipation (red) shifts (overtones 5−13) for adsorption/desorption of a bidentate flavin-ssDNA ligand (ligand Bi2, comprising 20 bases, equipped with flavins on both ends) at a dodecin DtE monolayer (prepared with 100% flavin surface coverage).

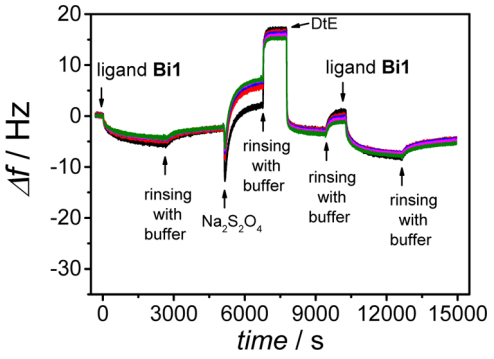

Figure 6. QCM frequency shifts (overtones 5−13) for adsorption/desorption of the bidentate flavin-dsDNA ligand Bi1 at a dodecin DtE monolayer (prepared with 100% flavin surface coverage), followed by disassembly of the sandwich-type surface architecture by flavin reduction using a solution of sodium dithionite, reassembly of the surface architecture by addition of apododecin DtE, and subsequent adsorption/desorption of the ligand Bi1.

Next we used the unique redox properties of dodecin in order to remove and reassemble the sandwich-type flavin-apododecin-flavin ligand array as shown in Figure 6. We first disassembled the surface architecture by flavin reduction (using a buffered sodium dithionite solution). This resulted in the release of the ligand and dodecin molecules. Thereafter the dodecin monolayer was restored by addition of a fresh apododecin DtE solution, and subsequently a new fraction of bidentate ligand **Bi1** was captured.

Using another flavin-dsDNA-modified chip we show in Figure 7 that it is even possible to replace one type of bidentate ligand by a different one, *i.e.*, to reprogram the surface architecture. In Figure 7A the QCM frequency and dissipation shifts measured during the adsorption (and subsequent rinsing with buffer) of ligand **Bi1** at a dodecin DtE monolayer (prepared with 100% flavin surface coverage) are shown. Thereafter

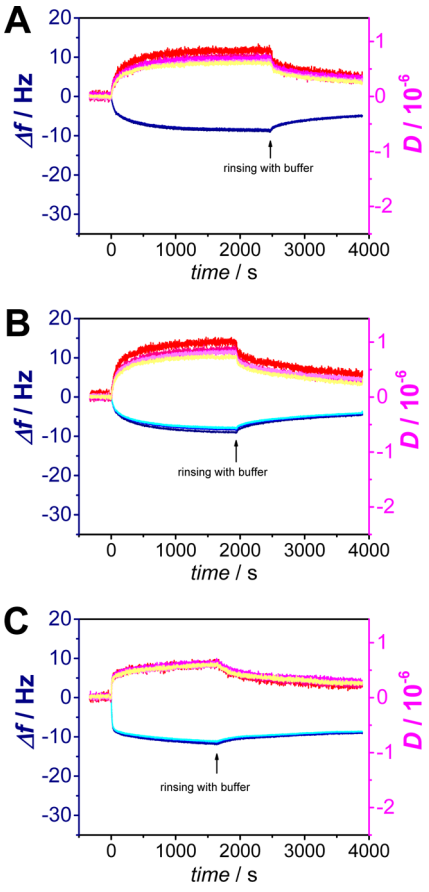

Figure 7. QCM frequency (blue) and dissipation (red) shifts (overtones 5−13) for adsorption/desorption of bidentate flavin-DNA ligands at three dodecin monolayers formed at the same flavin-DNA-modified chip. In (A) the ligand Bi1 was adsorbed followed by rinsing with buffer, before the ligand and the dodecin monolayer were released by chemical reduction with a buffered argon-saturated solution of sodium dithionite (100 mM). Thereafter a new dodecin monolayer was formed by adsorption of apododecin DtE, the measurement was restarted, and in (B) the adsorption/desorption kinetics of the ligand Bi1 were monitored a second time. Again the ligand and the dodecin monolayer were released, a new dodecin monolayer was formed, and the measurement was restarted before in (C) the adsorption/desorption kinetics of the ligand Bi2 were monitored.

the ligand and the DtE monolayer were released by reduction before a new DtE monolayer was formed. After the QCM measurement was restarted (in order to start the measurement exactly at $\Delta f = 0$ and $\Delta D = 0$) ligand **Bi1** was adsorbed a second time (see Figure 7B). Following this procedure ligand **Bi1** was removed again, and the dodecin monolayer was restored; before this time ligand **Bi2** was adsorbed at the same flavin-dsDNA modified chip (see Figure 7C). Hence, multiple reprogramming of a sandwich-type flavin-apododecin-flavin surface architecture using the same flavin-DNA tethers attached to a single chip was achieved. It is further worth noting that for the adsorption of the bidentate ligand **Bi2** the decrease in frequency is somewhat larger than for the bidentate ligand **Bi1** (both ligands were added at a concentration of 5 μM),

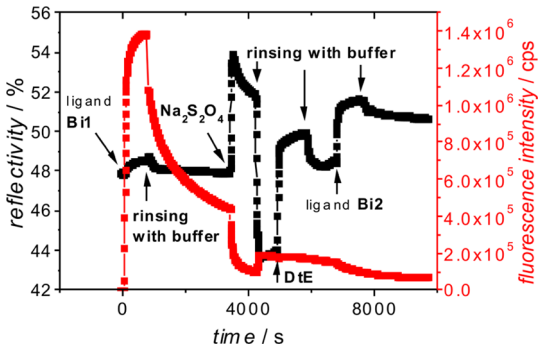

Figure 8. SPR and SPFS kinetic scan curves collected during adsorption/desorption of the fluorescent bidentate ligand Bi1 at a dodecin DtE monolayer (prepared with 100% flavin surface coverage), followed by disassembly of the sandwich-type surface architecture by flavin reduction using a solution of sodium dithionite, reassembly of the surface architecture by addition of apododecin DtE, and subsequent adsorption/desorption of the nonfluorescent bidentate ligand Bi2.

even though the molar mass of ligand **Bi2** is approximately half of that of ligand **Bi1**. Assuming that there is no significant difference in the contribution of trapped solvent molecules to the overall frequency shift,[23] this implies that more molecules of the flexible ligand **Bi2** can be adsorbed in comparison to ligand **Bi1**. Hence, in order to optimize the binding properties of multivalent flavin ligands, the flavins should be attached by rather long and flexible tethers. A more detailed comparison of the binding and unbinding kinetics of the ligands **Bi1** and **Bi2** including the determination of the individual binding affinities is provided in the Supporting Information.

Since in contrast to **Bi2** the ligand **Bi1** is Cy5-labeled, the fluorescence signal could be used as an additional readout channel. In Figure 8 the shifts in the SPR and SPFS kinetic scan curves during adsorption (and subsequent rinsing with buffer) of the fluorescent ligand **Bi1** at a dodecin DtE monolayer (prepared with 100% flavin surface coverage) followed by reprogramming the surface in order to obtain a surface modified with the nonfluorescent ligand **Bi2** are shown. By comparing the increase in the SPR signal during ligand binding for both ligands it can be seen that a larger amount of the flexible ligand **Bi2** can be adsorbed in comparison to ligand **Bi1** (as observed previously in the QCM-D measurements shown in Figure 7).

CONCLUSIONS

We have shown by QCM-D, SPR, and SPFS measurements how protein−DNA nanostructures can be generated, deleted, and reprogrammed on the same surface by exploiting multivalency and the redox properties of dodecin. Using flavin-modified dsDNA monolayers we have studied the binding properties of the multi-ligand-binding flavoprotein dodecin. The degree of multivalency depends strongly on the amount of flavins presented at the surface, which are

available for (apo)dodecin binding. At low flavin surface coverages (≤15%) the vast amount of dodecin molecules are captured only *via* a single binding event. Thus, it was possible to determine the previously unknown kinetic binding parameters, *i.e.*, the binding/unbinding rate constants (k_{on}/k_{off}) of a single apododecin-flavin-DNA complex by QCM measurements. The thermodynamic value of $K_{d(QCM)}$ = 580 nM calculated from $k_{on(QCM)} = 7.7 \times 10^3\ M^{-1} \cdot s^{-1}$ and $k_{off(QCM)} = 4.5 \times 10^{-3}\ s^{-1}$ is in good agreement with a dissociation constant of K_d = 400 nM, which has been determined previously by a fluorescence quenching binding assay (in solution).[15] Using SPFS and dynamic AFM-based single-molecule force spectroscopy as additional methods the values $k_{off(SPFS)} = 1.6 \times 10^{-3}\ s^{-1}$ and $k_{off(AFM)} = 6.8 \times 10^{-3}\ s^{-1}$ were obtained, which are in the same order of magnitude as the value from QCM. Even though the monovalent apododecin–flavin binding interaction ($K_{d(QCM)}$ = 580 nM and $k_{off(QCM)} = 4.5 \times 10^{-3}\ s^{-1}$) is orders of magnitude weaker than that of streptavidin–biotin ($K_d \approx 10$ fM and $k_{off} = 3.8 \times 10^{-6}\ s^{-1}$),[17,41−45] it is in the same range or even stronger than that of other prominent guest–host systems such as vancomycin–DADA (K_d = 1.6 μM and k_{off} = 31 s^{-1}),[34,48] concanavalin A–mannotriose (K_d = 250 nM and $k_{off} = 1.2 \times 10^{-2}\ s^{-1}$),[49] or further lectins,[50] cyclodextrin–adamantane (K_d = 22 μM and $k_{off} = 2 \times 10^3\ s^{-1}$),[39] or His-tag-$Ni^{2+}$–NTA ($K_d \approx 1\ \mu$M and $k_{off} \approx 2\ s^{-1}$).[51−53] In contrast to any of these guest–host systems the apododecin–flavin system can be easily and *reversibly* disassembled by ligand reduction, as we have shown by QCM and previously also by SPR measurements.[15]

Using the concept of multivalency, dodecin can be employed for the generation of rather stable sandwich-type flavin-apododecin-flavin surface architectures. Already bidentate flavin-DNA ligands bind to a dodecin layer (formed on top of a flavin-terminated DNA monolayer) sufficiently strong that the majority of the ligands remain captured after rinsing with buffer solution for 1 h. By comparing the two bidentate flavin-DNA model ligands **Bi1** and **Bi2**, we have shown that the more flexible arrangement of the flavin anchors in **Bi2** enhances the overall binding affinity. The formation of branched DNA molecules by hybridization of two or more flavin-modified ssDNA strands together with additionally functionalized ssDNA could be a simple and versatile access to functionalized multivalent ligands for applications in nano-biotechnology. Furthermore, we anticipate that due to the octahedral arrangement of the six dodecin binding pockets, dodecin is a promising building block for the generation of extended highly ordered three-dimensional protein–DNA nanostructures.

METHODS

Expression, Purification, and Refolding of Heterologously Expressed Apododecin Variants. The heterologous overexpression of N-terminally His6-tagged halopilic apododecin flavin binding variant triple E (tE; E45A delE50 delE51) was performed by transformation of the recombinant plasmid pDOD (pET22b(+), Novagen) with subcloned tE PCR product into chemocompetent BL21 (De3) *E. coli* strain. Purification and refolding processes were done as described previously.[12] Dodecameric dodecin was detected by size exclusion chromatography on a Superdex 200 10/300 GL column (GE Healthcare Life Sciences) equilibrated and eluted with buffer A. Since there might be some minor protein denaturation/precipitation upon long-term storage, the (apo)protein solutions were filtered through a cellulose 200 nm PVDF-membrane filter, hydrophilic, 0.22 μm (ROTH), prior to use.

Preparation of the Gold Substrates. SPR-Chip preparation: Gold substrates were prepared by vacuum evaporation of gold (48 nm layer thickness) onto cleaned glass slides (n_{BK7} = 1.515 at 633 nm), which were precoated with a thin titanium layer (1.5 nm) to improve adhesion. The gold substrates were freshly cleaned prior to use by treatment with piranha solution (3:1 concentrated H_2SO_4/30%H_2O_2, *CAUTION: piranha solution reacts violently with most organic materials and must be handled with extreme care*) for 5 min at room temperature and then rinsed with pure water.

For the QCM-D measurements standard sensor chips (QSX301, Q-Sense, Västra Frölunda, Sweden) with the following specifications were used: frequency 4.95 MHz ± 50 kHz, diameter 14 mm, thickness 0.3 mm, RMS surface roughness of electrode <3 nm. Before modification, the sensors were cleaned with a UV cleaner for 10 min, thereafter with basic piranha (1:1:5 of H_2O_2, 25% ammonia solution, MQ water) at 75 °C for 5 min, and again with UV treatment for 10 min.

Smooth gold substrates for the AFM force measurements and imaging were prepared by template stripping. After depositing a 50 nm gold layer on the "prime"-quality silicon wafer, used as a template, a glass slide was glued onto the gold surface using a two-component epoxy adhesive. After drying the glass slide bearing the gold layer was peeled off and used for further modification without cleaning.[54]

Deposition of DNA, Apododecin, and Ligands. The disulfide-modified ssDNA was adsorbed on the SPR, QCM-D, or AFM substrates in the following way. The DNA was dissolved in buffer A and adsorbed to the gold surface for 1 h. The 1,2-dithiane and flavin-modified ssDNA was used at a concentration of 2 μM, and the $(1,2\text{-dithiane})_3$-modified ssDNA at 5 μM, respectively. Efficient covalent tethering of the DNA strands to the gold surface was accomplished *via* the reaction of one or three dithiane groups with gold. The series of three disulfide groups substantially increased the overall binding strength, providing sufficient stability of the DNA monolayer on gold. After adsorption was completed, the surface was rinsed with buffer and MQ water. To replace nonspecifically adsorbed DNA strands and saturate free sites at the gold surface, in the next step a mixture of low-molecular-weight thiols was adsorbed.[55] Equimolar amounts of mercaptobutanol and mercaptopropionic acid, dissolved in water at 2 mM overall concentration, were adsorbed on the DNA-gold surface for 30 min followed by rinsing with MQ water. In order to obtain the flavin-dsDNA ligand modified surface, the surface-grafted ssDNA was hybridized with complementary flavin-modified ssDNA at 5 μM in buffer A. Dehybridization could be achieved by intense rinsing with pure water.[56] In all experiments apododecin DtE was added at a concentration of 5 μM. The mono- and bidentate flavin ligands were added at a concentration of 5 μM. Each step of surface modification was monitored by SPR or QCM-D measurements.

SPR and SPFS. For SPR and SPFS a commercially available setup from from Res-Tec (Resonant Technologies, Framersheim, Germany) was used. In order to estimate the maximum amount of apododecin that can be bound to a flavin-terminated DNA

monolayer, angular SPR scan curves were measured before and after apododecin DtE adsorption on three identically prepared SPR chips with a flavin surface coverage of 100%. From the shifts observed an average optical thickness ($n \times d$) of the apododecin monolayer of 3.9 nm was determined using the software Winspall, version 3.0.2.0 (Max Planck Institute of Polymer Research, Mainz, Germany).

QCM-D. QCM-D measurements were performed with a Q-sense E1 instrument (Q-Sense, Göteborg, Sweden), which was controlled by the QSoft 401 acquisition software. The QCM sensor crystals were cleaned in a BioForce ozone cleaner (BioForce, Ames, USA).

Dynamic AFM Force Spectroscopy and AFM Imaging. Dynamic AFM force spectroscopy and AFM imaging were performed using an Asylum MFP-3D Bio AFM (Asylum Research, Santa Barbara, CA, USA). In these measurements Olympus Biolever probes (Bruker OBL-10, Bruker AXS, Camarillo, CA, USA) with a nominal spring constant of 30 $pN \cdot nm^{-1}$ were used. Topographic images were acquired in tris-buffer using intermittent contact mode and contact mode. Calibration of the cantilevers was performed using the thermal noise method. The variation of the obtained values for the spring constant from the nominal values was in the range of ± 4 $pN \cdot nm^{-1}$. The sensitivity of the optical levers was obtained from force curves collected in several approach−retract cycles of the probe on a freshly cleaned glass surface. In the measurements a constant approach velocity of the cantilever toward the sample surface was used (0.5 $\mu m \cdot s^{-1}$), while the retract velocity was varied in the range from 0.05 to 3.5 $\mu m \cdot s^{-1}$. Upon contact with the substrate surface the cantilever deflection was kept low to prevent damage of the protein structure.[57] At each loading rate up to 2000 FD curves were recorded to acquire sufficient data for estimation of the most probable rupture force.

In order to measure the protein−ligand interactions, the gold-coated AFM tip was modified with the flavin-ssDNA ligand. Prior to modification the AFM probe was rinsed with 2-propanol and pure water. Afterward, it was immersed in a 2 μM solution of the 5′-flavin- and 3′-dithiol-modified ssDNA for 1 h according to the procedure described above for the modification of gold substrates. The gold-coated substrate surface used for AFM measurements was modified with the 5′-flavin- and 3′-dithiol-modified ssDNA as described above and apododecin DtE was immobilized on this surface *via* binding the flavin ligands. For this purpose DtE was added at a concentration of 20 nM (concentration of the dodecameric apoprotein) in buffer A solution. The low adsorption density enabled the formation of multiple linkages between a single apododecin molecule and the surface-bound flavin ligands oriented almost parallel to each other, increasing the binding strength between apododecin and the flavin-modified surface. For a system containing parallel bond attachment the rupture force increases with the number of bonds involved in this linkage.[39,58−60] Thus, it was assumed that in the measurements the rupture of the apododecin−flavin tip bonds prevail over apododecin−flavin surface rupture.

Conflict of Interest: The authors declare no competing financial interest.

Acknowledgment. We thank Dr. Roman Sheparovych and Dr. Daniel Wesner for experimental support. This work has received funding from the European Research Council under the European Community's Seventh Framework Programme (FP7/2007-2013)/ERC Grant agreement no. 240544, from the country North Rhine-Westphalia, the University of Siegen, and the Deutsche Forschungsgemeinschaft (DFG grant no. INST 221/87-1 FUGG).

Supporting Information Available: This material is available free of charge *via* the Internet at http://pubs.acs.org.

REFERENCES AND NOTES

1. Mendes, P. M. Stimuli-Responsive Surfaces for Bio-Applications. *Chem. Soc. Rev.* **2008**, *37*, 2512–2529.
2. Lahann, J.; Mitragotri, S.; Tran, T.-N.; Kaido, H.; Sundaram, J.; Choi, I. S.; Hoffer, S.; Somorjai, G. A.; Langer, R. A Reversibly Switching Surface. *Science* **2003**, *299*, 371–374.
3. Russell, T. P. Materials Science: Soft Surfaces: Surface-Responsive Materials. *Science* **2002**, *297*, 964–967.
4. Pranzetti, A.; Preece, J. A.; Mendes, P. M. Stimuli-Responsive Surfaces in Biomedical Applications. In *Intelligent Stimuli-Responsive Materials: From Well-Defined Nanostructures to Applications*; Li, Q., Ed.; Wiley-VCH, 2013; pp 377−422.
5. Wischerhoff, E.; Badi, N.; Lutz, J.-F.; Laschewsky, A. Smart Bioactive Surfaces. *Soft Matter* **2010**, *6*, 705–713.
6. Lee, I. Molecular Self-Assembly: Smart Design of Surface and Interface *via* Secondary Molecular Interactions. *Langmuir* **2013**, *29*, 2476–2489.
7. Yang, Y.-W.; Sun, Y.-L.; Song, N. Switchable Host-Guest Systems on Surfaces. *Acc. Chem. Res.* **2014**, *47*, 1950–1960.
8. Taskinen, B.; Zauner, D.; Lehtonen, S. I.; Koskinen, M.; Thomson, C.; Kahkonen, N.; Kukkurainen, S.; Maatta, J. A. E.; Ihalainen, T. O.; Kulomaa, M. S.; *et al*. Switchavidin: Reversible Biotin-Avidin-Biotin Bridges with High Affinity and Specificity. *Bioconjugate Chem.* **2014**, *25*, 2233–2243.
9. Grininger, M.; Nöll, G.; Trawöger, S.; Sinner, E.-K.; Oesterhelt, D. Electrochemical Switching of the Flavoprotein Dodecin at Gold Surfaces Modified by Flavin-DNA Hybrid Linkers. *Biointerphases* **2008**, *3*, 51–58.
10. Grininger, M.; Seiler, F.; Zeth, K.; Oesterhelt, D. Dodecin Sequesters FAD in Closed Conformation from the Aqueous Solution. *J. Mol. Biol.* **2006**, *364*, 561–566.
11. Grininger, M.; Staudt, H.; Johansson, P.; Wachtveitl, J.; Oesterhelt, D. Dodecin Is the Key Player in Flavin Homeostasis of Archaea. *J. Biol. Chem.* **2009**, *284*, 13068–13076.
12. Grininger, M.; Zeth, K.; Oesterhelt, D. Dodecins: A Family of Lumichrome Binding Proteins. *J. Mol. Biol.* **2006**, *357*, 842–857.
13. Nöll, G.; Trawöger, S.; von Sanden-Flohe, M.; Dick, B.; Grininger, M. Blue-Light-Triggered Photorelease of Active Chemicals Captured by the Flavoprotein Dodecin. *ChemBioChem* **2009**, *10*, 834–837.
14. Staudt, H.; Oesterhelt, D.; Grininger, M.; Wachtveitl, J. Ultrafast Excited-State Deactivation of Flavins Bound to Dodecin. *J. Biol. Chem.* **2012**, *287*, 17637–17644.
15. Yu, Y.; Heidel, B.; Parapugna Tamara, L.; Wenderhold-Reeb, S.; Song, B.; Schönherr, H.; Grininger, M.; Nöll, G. The Flavoprotein Dodecin as a Redox Probe for Electron Transfer through DNA. *Angew. Chem., Int. Ed.* **2013**, *52*, 4950–4953.
16. Nöll, T.; Nöll, G. Strategies for "Wiring" Redox-Active Proteins to Electrodes and Applications in Biosensors, Biofuel Cells, and Nanotechnology. *Chem. Soc. Rev.* **2011**, *40*, 3564–3576.
17. Jung, L. S.; Nelson, K. E.; Stayton, P. S.; Campbell, C. T. Binding and Dissociation Kinetics of Wild-Type and Mutant Streptavidins on Mixed Biotin-Containing Alkylthiolate Monolayers. *Langmuir* **2000**, *16*, 9421–9432.
18. Georgiadis, R.; Peterlinz, K. P.; Peterson, A. W. Quantitative Measurements and Modeling of Kinetics in Nucleic Acid Monolayer Films Using SPR Spectroscopy. *J. Am. Chem. Soc.* **2000**, *122*, 3166–3173.
19. Liu, Y.; Shen, L. From Langmuir Kinetics to First- and Second-Order Rate Equations for Adsorption. *Langmuir* **2008**, *24*, 11625–11630.
20. Marczewski, A. W. Analysis of Kinetic Langmuir Model. Part I: Integrated Kinetic Langmuir Equation (IKL): A New Complete Analytical Solution of the Langmuir Rate Equation. *Langmuir* **2010**, *26*, 15229–15238.
21. Liepold, P.; Kratzmueller, T.; Persike, N.; Bandilla, M.; Hinz, M.; Wieder, H.; Hillebrandt, H.; Ferrer, E.; Hartwich, G. Electrically Detected Displacement Assay (Edda): A Practical Approach to Nucleic Acid Testing in Clinical or Medical Diagnosis. *Anal. Bioanal. Chem.* **2008**, *391*, 1759–1772.
22. Su, Q.; Wesner, D.; Schönherr, H.; Nöll, G. Molecular Beacon Modified Sensor Chips for Oligonucleotide Detection with Optical Readout. *Langmuir* **2014**, *30*, 14360–14367.
23. Reviakine, I.; Johannsmann, D.; Richter, R. P. Hearing What You Cannot See and Visualizing What You Hear: Interpreting Quartz Crystal Microbalance Data from Solvated Interfaces. *Anal. Chem.* **2011**, *83*, 8838–8848.

24. Tellechea, E.; Johannsmann, D.; Steinmetz, N. F.; Richter, R. P.; Reviakine, I. Model-Independent Analysis of QCM Data on Colloidal Particle Adsorption. *Langmuir* **2009**, *25*, 5177–5184.
25. Johannsmann, D.; Reviakine, I.; Rojas, E.; Gallego, M. Effect of Sample Heterogeneity on the Interpretation of QCM(-D) Data: Comparison of Combined Quartz Crystal Microbalance/Atomic Force Microscopy Measurements with Finite Element Method Modeling. *Anal. Chem.* **2008**, *80*, 8891–8899.
26. Johannsmann, D.; Reviakine, I.; Richter, R. P. Dissipation in Films of Adsorbed Nanospheres Studied by Quartz Crystal Microbalance (QCM). *Anal. Chem.* **2009**, *81*, 8167–8176.
27. Bingen, P.; Wang, G.; Steinmetz, N. F.; Rodahl, M.; Richter, R. P. Solvation Effects in the Quartz Crystal Microbalance with Dissipation Monitoring Response to Biomolecular Adsorption. A Phenomenological Approach. *Anal. Chem.* **2008**, *80*, 8880–8890.
28. Papadakis, G.; Tsortos, A.; Bender, F.; Ferapontova, E. E.; Gizeli, E. Direct Detection of DNA Conformation in Hybridization Processes. *Anal. Chem.* **2012**, *84*, 1854–1861.
29. Tsortos, A.; Papadakis, G.; Gizeli, E. Shear Acoustic Wave Biosensor for Detecting DNA Intrinsic Viscosity and Conformation: A Study With QCM-D. *Biosens. Bioelectron.* **2008**, *24*, 836–841.
30. Höök, F.; Kasemo, B.; Nylander, T.; Fant, C.; Sott, K.; Elwing, H. Variations in Coupled Water, Viscoelastic Properties, and Film Thickness of A Mefp-1 Protein Film during Adsorption and Cross-Linking: A Quartz Crystal Microbalance with Dissipation Monitoring, Ellipsometry, and Surface Plasmon Resonance Study. *Anal. Chem.* **2001**, *73*, 5796–5804.
31. Mammen, M.; Chio, S.-K.; Whitesides, G. M. Polyvalent Interactions in Biological Systems: Implications for Design and Use of Multivalent Ligands and Inhibitors. *Angew. Chem., Int. Ed.* **1998**, *37*, 2755–2794.
32. Bastings, M. M. C.; Helms, B. A.; van Baal, I.; Hackeng, T. M.; Merkx, M.; Meijer, E. W. From Phage Display to Dendrimer Display: Insights into Multivalent Binding. *J. Am. Chem. Soc.* **2011**, *133*, 6636–6641.
33. Badjic, J. D.; Nelson, A.; Cantrill, S. J.; Turnbull, W. B.; Stoddart, J. F. Multivalency and Cooperativity in Supramolecular Chemistry. *Acc. Chem. Res.* **2005**, *38*, 723–732.
34. Rao, J.; Lahiri, J.; Isaacs, L.; Weis, R. M.; Whitesides, G. M. A Trivalent System from Vancomycin·D-Ala-D-Ala with Higher Affinity Than Avidin·Biotin. *Science* **1998**, *280*, 708–711.
35. Cabanas-Danes, J.; Rodrigues, E. D.; Landman, E.; van Weerd, J.; van Blitterswijk, C.; Verrips, T.; Huskens, J.; Karperien, M.; Jonkheijm, P. A Supramolecular Host-Guest Carrier System for Growth Factors Employing VHH Fragments. *J. Am. Chem. Soc.* **2014**, *136*, 12675–12681.
36. Evans, E. Energy Landscapes of Biomolecular Adhesion and Receptor Anchoring at Interfaces Explored with Dynamic Force Spectroscopy. *Faraday Discuss.* **1999**, *111*, 1–16.
37. Alessandrini, A.; Facci, P. AFM: A Versatile Tool in Biophysics. *Meas. Sci. Technol.* **2005**, *16*, R65–R92.
38. Strunz, T.; Oroszlan, K.; Schafer, R.; Guntherodt, H.-J. Dynamic Force Spectroscopy of Single DNA Molecules. *Proc. Natl. Acad. Sci. U.S.A.* **1999**, *96*, 11277–11282.
39. Gomez-Casado, A.; Dam, H. H.; Yilmaz, M. D.; Florea, D.; Jonkheijm, P.; Huskens, J. Probing Multivalent Interactions in a Synthetic Host-Guest Complex by Dynamic Force Spectroscopy. *J. Am. Chem. Soc.* **2011**, *133*, 10849–10857.
40. Jonkheijm, P.; Weinrich, D.; Schroeder, H.; Niemeyer, C. M.; Waldmann, H. Chemical Strategies for Generating Protein Biochips. *Angew. Chem., Int. Ed.* **2008**, *47*, 9618–9647.
41. Niemeyer, C. M. Semisynthetic DNA-Protein Conjugates for Biosensing and Nanofabrication. *Angew. Chem., Int. Ed.* **2010**, *49*, 1200–1216.
42. Grunwald, C. A Brief Introduction to the Streptavidin-Biotin System and Its Usage in Modern Surface Based Assay. *Z. Phys. Chem.* **2008**, *222*, 789–821.
43. Müller, W.; Ringsdorf, H.; Rump, E.; Wildburg, G.; Zhang, X.; Angermaier, L.; Knoll, W.; Liley, M.; Spinke, J. Attempts to Mimic Docking Processes of the Immune System: Recognition-Induced Formation of Protein Multilayers. *Science* **1993**, *262*, 1706–1708.
44. Su, X.; Wu, Y.-J.; Robelek, R.; Knoll, W. Surface Plasmon Resonance Spectroscopy and Quartz Crystal Microbalance Study of Streptavidin Film Structure Effects on Biotinylated DNA Assembly and Target DNA Hybridization. *Langmuir* **2005**, *21*, 348–353.
45. Laitinen, O. H.; Hytonen, V. P.; Nordlund, H. R.; Kulomaa, M. S. Genetically Engineered Avidins and Streptavidins. *Cell. Mol. Life Sci.* **2006**, *63*, 2992–3017.
46. Huskens, J.; Mulder, A.; Auletta, T.; Nijhuis, C. A.; Ludden, M. J. W.; Reinhoudt, D. N. A Model for Describing the Thermodynamics of Multivalent Host-Guest Interactions at Interfaces. *J. Am. Chem. Soc.* **2004**, *126*, 6784–6797.
47. Perl, A.; Gomez-Casado, A.; Thompson, D.; Dam, H. H.; Jonkheijm, P.; Reinhoudt, D. N.; Huskens, J. Gradient-Driven Motion of Multivalent Ligand Molecules along a Surface Functionalized with Multiple Receptors. *Nat. Chem.* **2011**, *3*, 317–322.
48. Popieniek, P. H.; Pratt, R. F. Kinetics and Mechanism of Binding of Specific Peptides to Vancomycin and Other Glycopeptide Antibiotics. *J. Am. Chem. Soc.* **1991**, *113*, 2264–2270.
49. Mori, T.; Toyoda, M.; Ohtsuka, T.; Okahata, Y. Kinetic Analyses for Bindings of Concanavalin A to Dispersed and Condensed Mannose Surfaces on a Quartz Crystal Microbalance. *Anal. Biochem.* **2009**, *395*, 211–216.
50. Lis, H.; Sharon, N. Lectins: Carbohydrate-Specific Proteins That Mediate Cellular Recognition. *Chem. Rev.* **1998**, *98*, 637–674.
51. Nieba, L.; Nieba-Axmann, S. E.; Persson, A.; Hamalainen, M.; Edebratt, F.; Hansson, A.; Lidholm, J.; Magnusson, K.; Karlsson, A. F.; Pluckthun, A. BIACORE Analysis of Histidine-Tagged Proteins Using a Chelating NTA Sensor Chip. *Anal. Biochem.* **1997**, *252*, 217–228.
52. Verbelen, C.; Gruber, H. J.; Dufrene, Y. F. The NTA-His6 Bond Is Strong Enough for AFM Single-Molecular Recognition Studies. *J. Mol. Recognit.* **2007**, *20*, 490–494.
53. Lata, S.; Reichel, A.; Brock, R.; Tampe, R.; Piehler, J. High-Affinity Adaptors for Switchable Recognition of Histidine-Tagged Proteins. *J. Am. Chem. Soc.* **2005**, *127*, 10205–10215.
54. Song, B.; Walczyk, W.; Schönherr, H. Contact Angles of Surface Nanobubbles on Mixed Self-Assembled Monolayers with Systematically Varied Macroscopic Wettability by Atomic Force Microscopy. *Langmuir* **2011**, *27*, 8223–8232.
55. Wong, E. L. S.; Chow, E.; Gooding, J. J. DNA Recognition Interfaces: The Influence of Interfacial Design on the Efficiency and Kinetics of Hybridization. *Langmuir* **2005**, *21*, 6957–6965.
56. Nöll, G.; Su, Q.; Heidel, B.; Yu, Y. A Reusable Sensor for the Label-Free Detection of Specific Oligonucleotides by Surface Plasmon Fluorescence Spectroscopy. *Adv. Healthcare Mater.* **2014**, *3*, 42–46.
57. Guo, S.; Li, N.; Lad, N.; Ray, C.; Akhremitchev, B. B. Mechanical Distortion of Protein Receptor Decreases the Lifetime of a Receptor-Ligand Bond. *J. Am. Chem. Soc.* **2010**, *132*, 9681–9687.
58. Evans, E. Probing the Relation between Force-Lifetime- and Chemistry in Single Molecular Bonds. *Annu. Rev. Biophys. Biomol. Struct.* **2001**, *30*, 105–128.
59. Gu, C.; Kirkpatrick, A.; Ray, C.; Guo, S.; Akhremitchev, B. B. Effects of Multiple-Bond Ruptures in Force Spectroscopy Measurements of Interactions between Fullerene C60 Molecules in Water. *J. Phys. Chem. C* **2008**, *112*, 5085–5092.
60. Guo, S.; Ray, C.; Kirkpatrick, A.; Lad, N.; Akhremitchev, B. B. Effects of Multiple-Bond Ruptures on Kinetic Parameters Extracted from Force Spectroscopy Measurements: Revisiting Biotin-Streptavidin Interactions. *Biophys. J.* **2008**, *95*, 3964–3976.